52 KSME Journal, Vol. 1, No. 1, pp. 52~59, 1987.

COMPUTATIONAL STUDY OF FLOW IN A CURVED PIPE WITH CIRCULAR CROSS SECTION

Susumu Shirayama* and Kunio Kuwahara**

(Received March 10, 1987)

Laminar imcompressible flows in a circular sectioned pipe were investigated by seeking numerical solutions to the Navier-Stokes equations. Three semi-circular pipes of radius ratios 0.05, 0.143 and 0.148 were studied. These calculations covered the Dean number ranging from 183 to 3847. In the range of low and medium Dean numbers, a steady-state solution was obtained; when the Dean number was high, a three-dimensional separation and the associated secondary flow were clearly observed far downstream near the outlet. Extensive flow visualizations were made to depict the computed results.

Key Words : Incompressible-Flow Computation, Pipe Flow, Dean Number, Computational Flow Visualization

1. INTRODUCTION

The flow in a curved pipe has been of considerable interest to the fluid mechanicians. Among others, a proper understanding of the complicated secondary motions in the cross-sectional plane is necessary for design and operation of a multitude of fluid machinery. One important parameter for this flow is the Dean number, which can be defined by the curvature of the pipe and the Reynolds number. When the Dean number is relatively low (say, less than 700), the structure of the secondary flow has been examined previously by experimental as well as analytical and theoretical investigations. The existence of the secondary flow has been verified by the previous studies. Some experiments demonstrated bifurcation or separation of the secondary flow (see, Agrawal et al., 1978). Although some numerical results were suggestive of such phenomena (Nandakumar et al., 1982; Humphrey et al., 1985), the majority of the numerical studies were unable to describe cleary such interesting flow features. This difficulty in the numerical works is believed to stem from the fact that the numerical models have mostly relied on approximate equations. When the Dean number is high, the flow may become unsteady, and separation may take place. For a comprehensive depiction of the flow, therefore, it will be highly desirable to solve the full, time-dependent Navier-Stokes equations.

In the present paper, the incompressible Navier-Stokes equations were solved by using a sufficient number of grid points. Computations were made for the flow in a circular-sectioned pipe with straight inlet and outlet. The flow details were illustrated by an extensive use of the computational flow visualization techniques incorporating a three-dimensional color graphics system.

2. METHOD OF APPROACH

A finite-difference procedure was applied to solve the three-dimensional incompressible Navier-Stokes equations written in a generalized coordinate system. In order to treat the pressure, the Helmholtz decomposition was adopted. (Chorin, 1968; Takami & Kuwahara, 1974) The resulting pressure equation was solved by the method of successive over-relaxation. The Euler implicit scheme was selected for the time integration. All the spatial derivatives except the nonlinear terms were apporoximated by central differences.

* The Institute of Computational Fluid Dynamics, 1-22-3 Haramachi, Meguro-ku, Tokyo 152, Japan

** The Institute of Space and Astronautical Science, Komaba, Meguro-ku, Tokyo 153, Japan

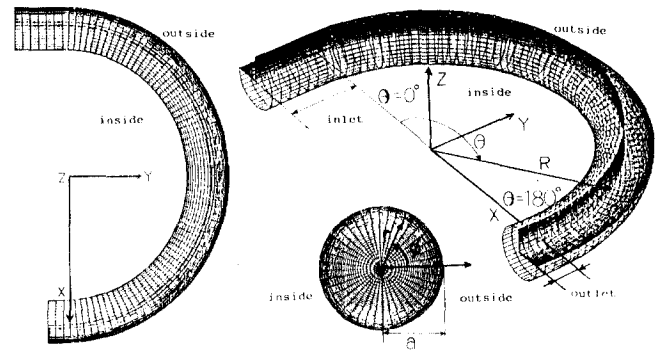

Fig. 1 Grid system.

The nonlinear terms were approximated by a third-order upwind scheme(Kawamura & Kuwahara, 1985; Himeno et al., 1985).

The computations were performed on the Japanese super-computers, i.e., Fujitsu VP 200, VP 400 and NEC SX/2.

The grid layout is shown in Fig. 1. The equations were solved in the generalized coordinate system. Along the symmetric axis, the equations were solved in the cartesian coordinate system. For an effective description of the computed results, as was done by the previous studies, a cylindrical coordinate frame (r,θ,z) will be introduced to cleary illuminate the flow details.

3. RESULTS

In the first, a case of low Dean number was dealt with. The Reynolds number was Re=484, a/R=1/7, and the Dean number De=183, and number of grid points was $79\times25\times35$. Figure 2 exemplifies the velocity distributions and pressure

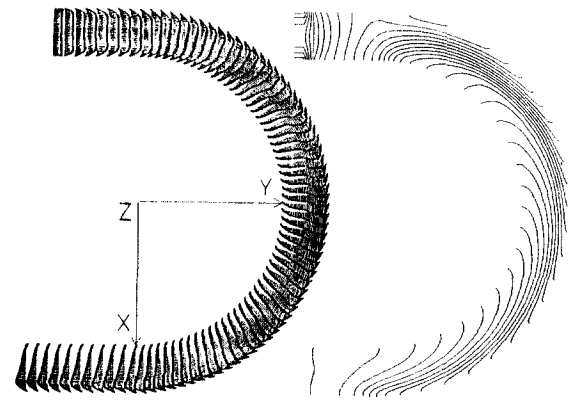

Fig. 2 Velocity vectors and pressure contours in the Symmetric plane.

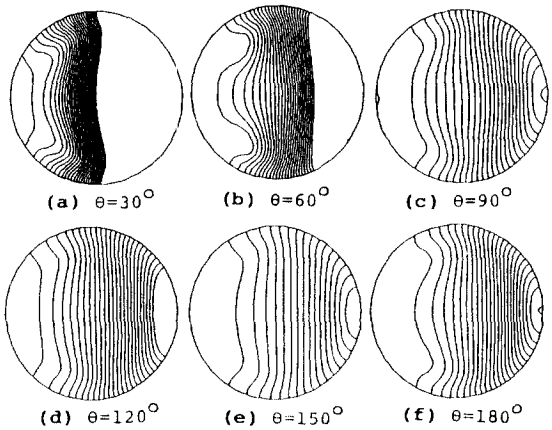

Fig. 3 Pressure contours in a cross-sectional plane.

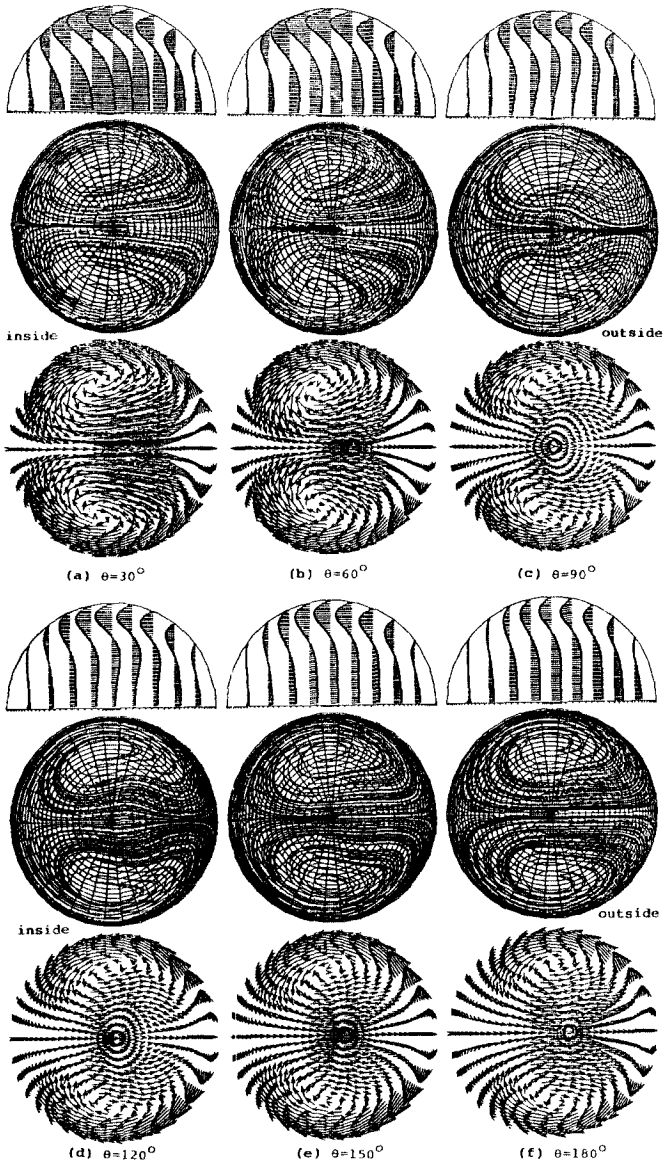

Fig. 4 Velocity profiles(ϕcomponent), particle paths in a cross-sectional plane and velocity vectors (Re=484, De=183, a/R=1/7).

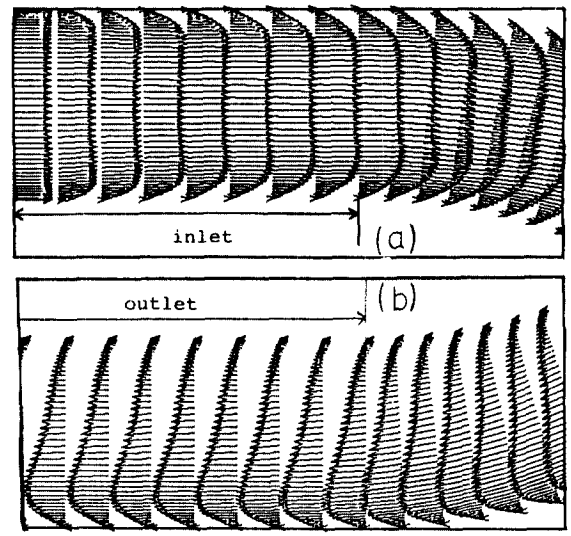

Fig. 5 Velocity vectors near the inlet.

contours in the symmetrical plane. Pressure contours at different cross sections are shown in Fig. 3. The profiles of the ϕ-component of velocity, the particle paths, and the velocity vectors in the cross-sectional plane are exhibited in Fig. 4. Two recirculating regions, which are symmetric about the center line, are discernible. These are referred to as the secondary flow. Figure 5 shows the velocity distributions near the inlet and outlet. The streamwise velocity profiles at t=100 are plotted in Fig. 6 (the upper diagrams), and, for comparison purposes, the experimetal data (Agrawal et al., 1978) are included (the lower diagrams). The profiles of the θ-component of the secondary flow are presented in Fig. 7.

In the second phase, three cases of computations were made, encompassing the range of moderate Dean numbers;

(i) Re=2527, a/R=1/20, De=565, grid points 119×34×43;
(ii) Re=3032, a/R=1/20, De=678, grid points 119×34×43;
(iii) Re=1764, a/R=1/7, De=678, grid points 99×34×38.

Figures 8 and 9 display the velocity profiles (the θ-component), particle paths, and velocity vectors in the cross-sectional plane at t=0. It is now clear that a distinctive flow pattern, known as the four-vortex solution (Nandakumar et al., 1982), emerges. The streamwise velocity profiles at t=100 are depicted in Fig. 10. Double velocity maxima along some lines are apparent in the figures. The computational results are in qualitative agreement with the experimental data. The profiles of the secondary flows are shown in Fig. 11 which includes the corresponding experimental results. The isovels of the streamwise velocity are plotted in Fig. 12. Comparisons demonstrating the agreement between the numerical predictions and the experimental measurements are illustrated in Fig. 13 for the flow at 83° from the entry when the Dean number is 565.

The highest Dean number for which the computations were conducted was Re=10,000, a/R=0.148, Dean=3847, grid points 161×35×41. Figure 14 contains the plots for velocity distributions and pressure contours in the symmetry plane. Figure 15 depicts the pressure contours at t=100 in some cross-sectional planes. The particle paths and the velocity vectors in a cross sectional plane at t=75 are shown in Fig. 16. Fugure 17 shows the velocity profiles of the secondary flows, particle paths, and velocity vectors in a cross-sectional plane at t=100.

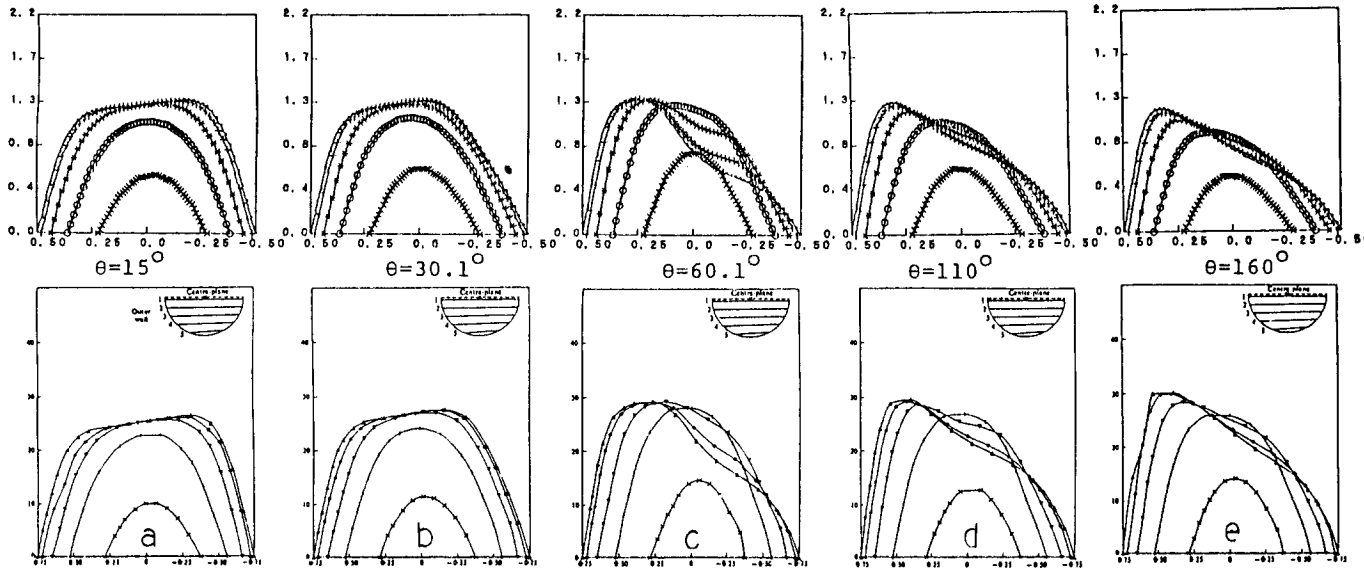

Fig. 6 Streamwise velocity profiles. The lower figures: experiment of Agrawal et al.(1978).

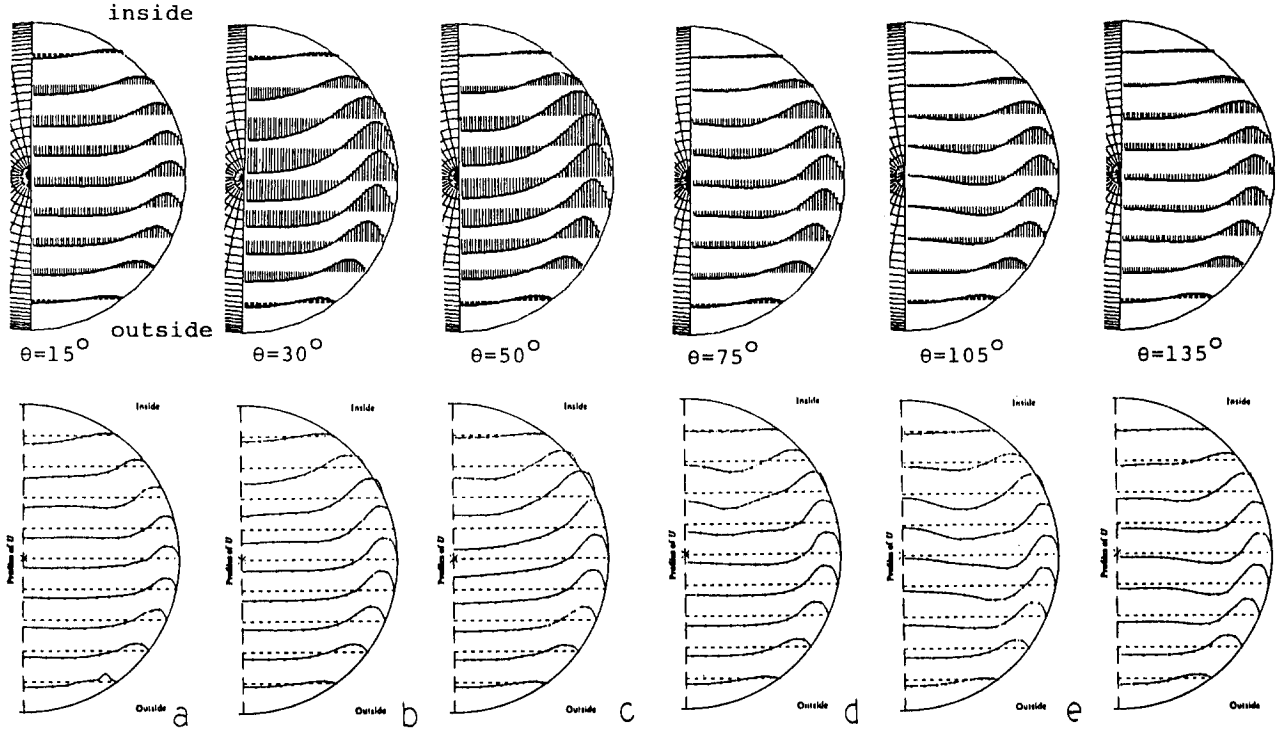

Fig. 7 Secondary-velocity profiles (ϕ component). The lower figures: experiment of Agrawal et al.(1978).

The question of whether a two-or a four-vortex solution is obtainable may be qualitatively answered as follows. It is believed to be largely dependent on the response of a viscous fluid element to the unbalance between the centripetal acceleration and the cross-sectional pressure gradient induced by the lateral curvature of the main flow. However, it appears that some of the recirculation regions are due to the separation of the main flow. Figure 18 exhibits the temporal development of the velocity profiles near the outlet. The main flow is seen to separate at t=100. Figure 19 displays the pressure contours on the inside wall and the equi-pressure surfaces near the outlet. The computed oil flow patterns are sketched in Fig. 20.

In an effort to examine the details of the three-dimensional separation, the flow field at t=100 is scrutinized by the aid of computational flow visualization techniques. Figure 21 is typical of the computed oil flow patterns and particle paths in a cross-sectional plane. Figure 22 displays the computed oil flow patterns at a location slightly downstream of the point used for Fig. 20 (b). The vortical structures are clearly identifiable by tracing the vortex lines; the same method was employed by Kim & Moin(1986). Figure 23 represents the vortex lines, which enable us to see the instantaneous vortical structure. The location for the vortex lines in Fig. 23 (a) is slightly upstream of the one for Fig. 23 (b).

It may not be possible to attain a fundamental understanding of the physics of these complex flows without efficient visualizations techniques, both hardware and software.

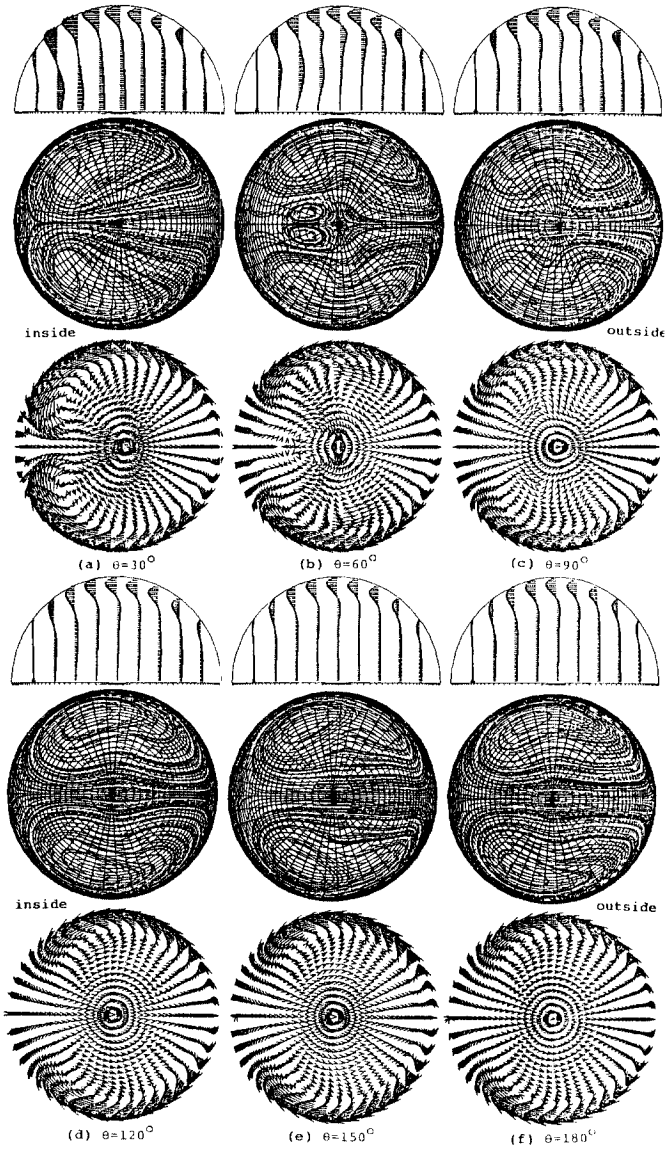

Fig. 8 Velocity profiles (ϕcomponent), particle paths in a cross-sectional plane and velocity vectors (Re=3032, De=678, a/R=1/20).

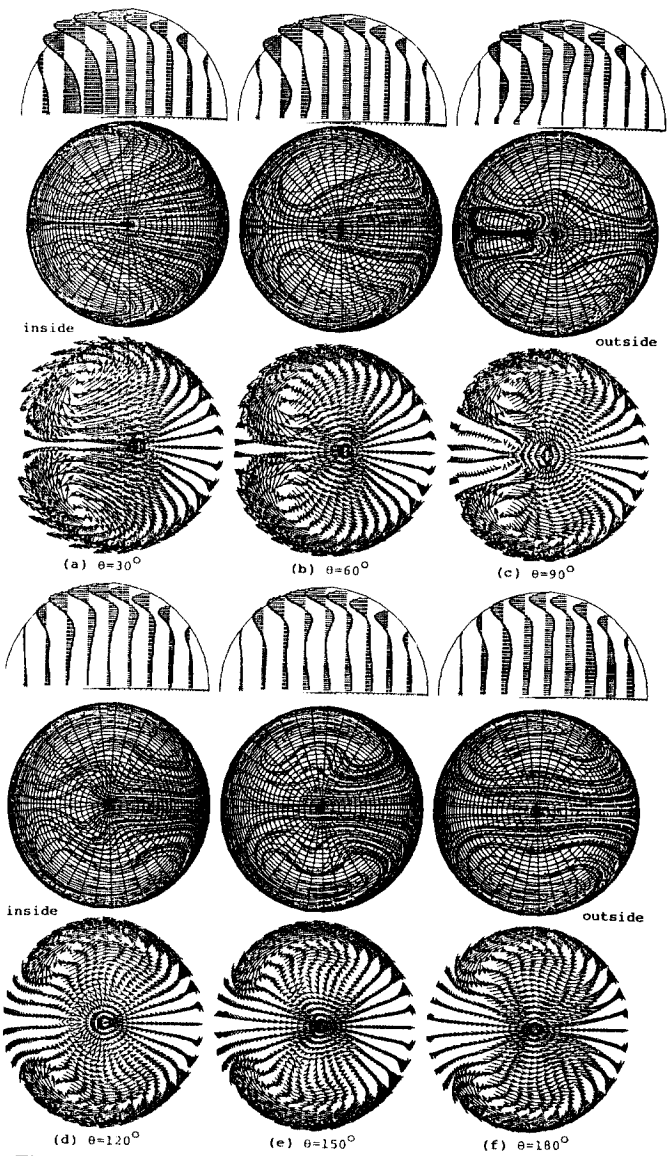

Fig. 9 Velocity profiles (ϕ component), particle paths in a cross-sectional plane and velocity vectors (Re=1764, De=678, a/R=1/7).

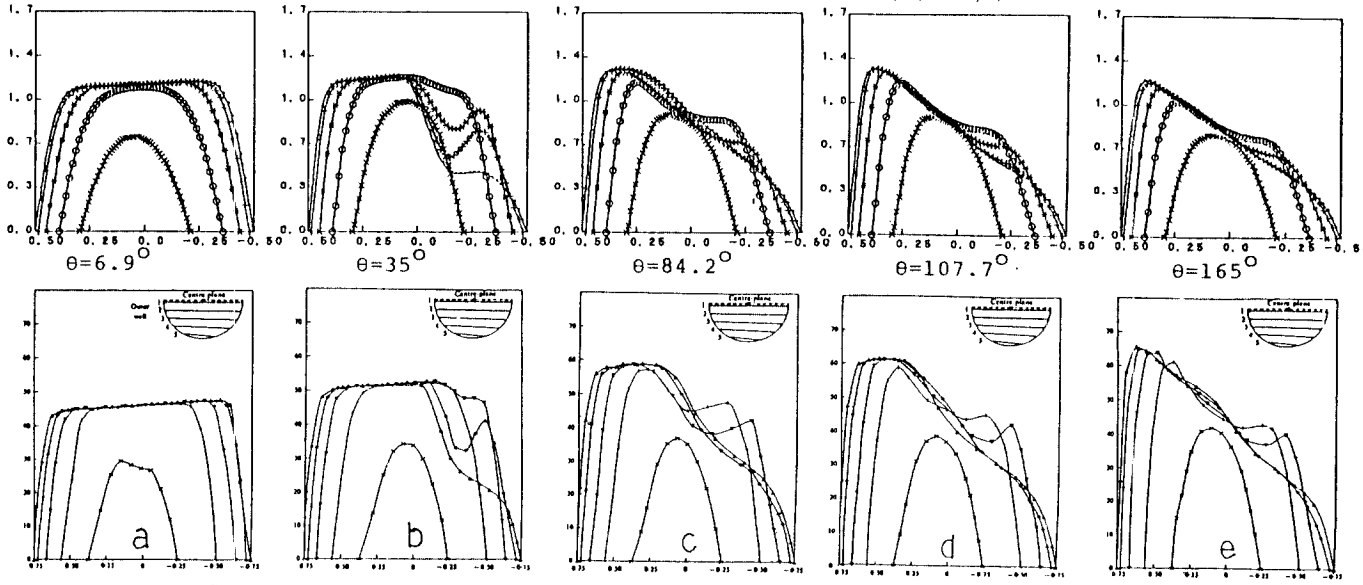

Fig. 10 Streamwise velocity profiles; De=565, a/R=1/20. The lower figures: experiment of Agrawal et al.(1978).

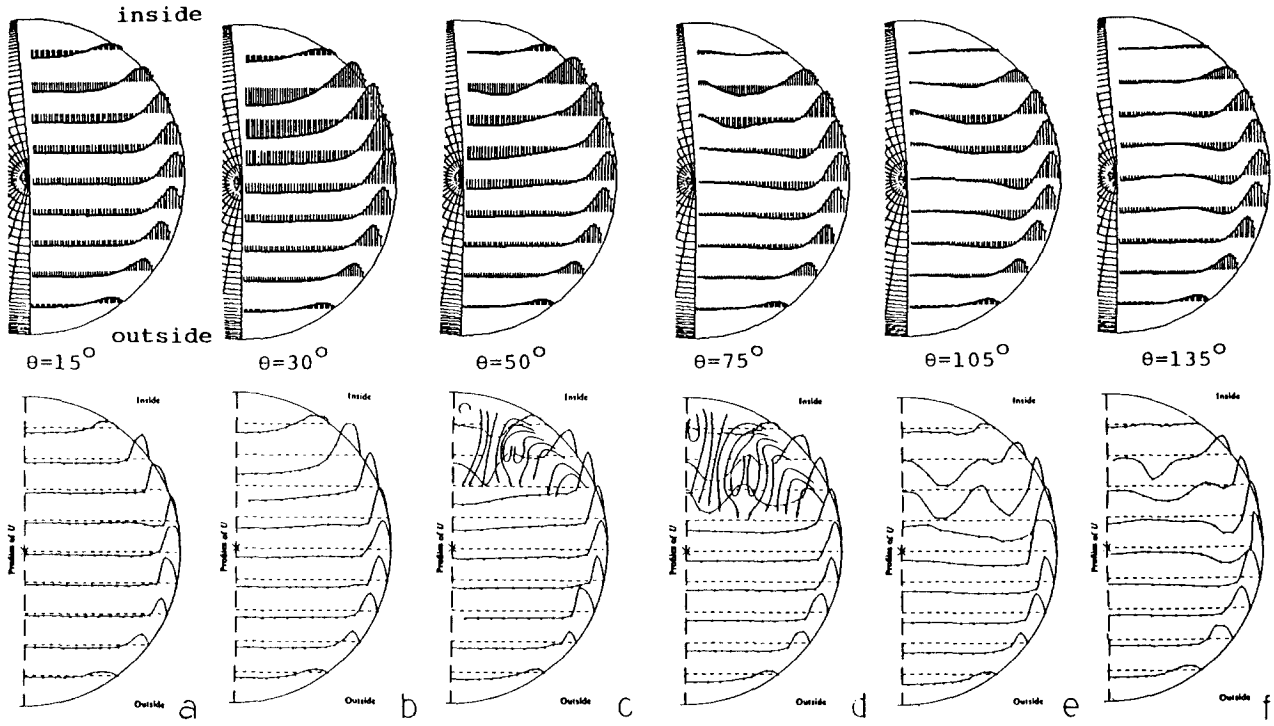

Fig. 11 Secondary-velocity profiles (ϕ component); De=678, a/R=1/7. The lower figures: experiment of Agrawal et al.(1978).

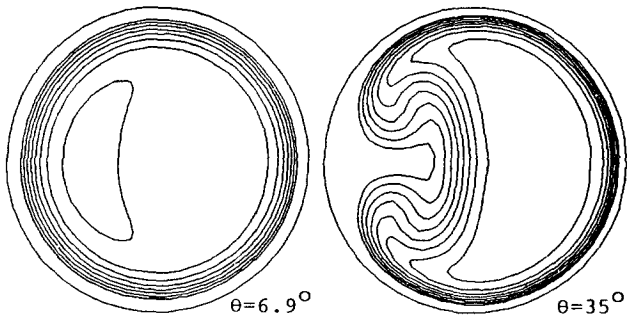

Fig. 12 Streamwise-velocity contours; De=565, a/R=1/20.

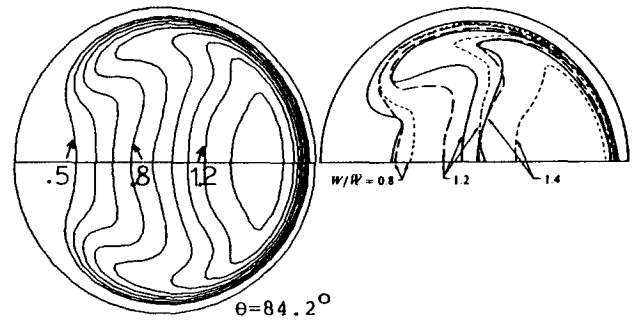

Fig. 13 Streamwise-velocity contours; De=565, a/R=1/20, θ=84.2°.
———, Talbot et al.;
– – – –, Humphrey et al.;
·····, Soh.

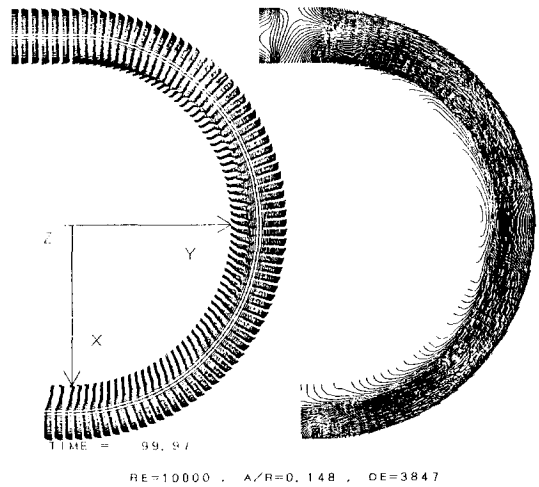

Fig. 14 Velocity vectors and pressure contours in the symmetric plane.

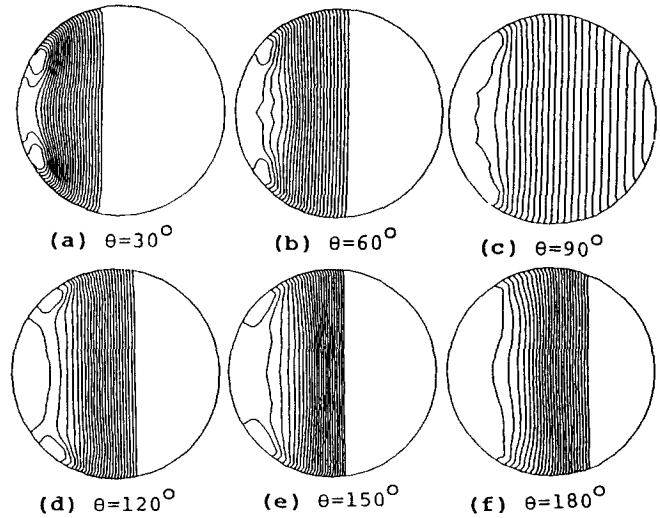

Fig. 15 Pressure contours in a cross-sectional plane.

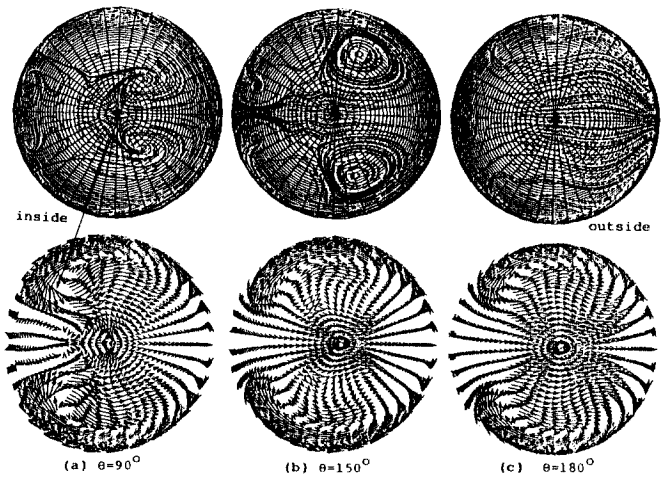

Fig. 16 Particle paths in a cross-sectional plane and velocity vectors at t=75. (Re=10000, De=3847, a/R=0.148)

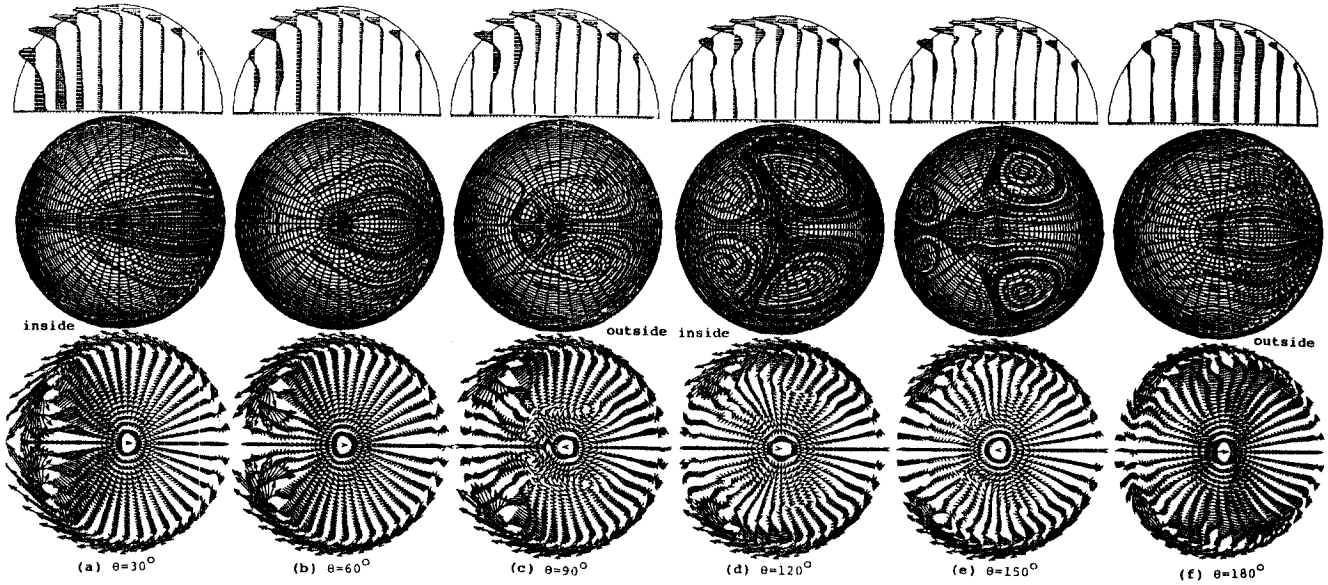

Fig. 17 Velocity profiles (ϕ component), particle paths in a cross-sectional plane and velocity vectors at t=100. (Re=10000, De=3847, a/R=0.148)

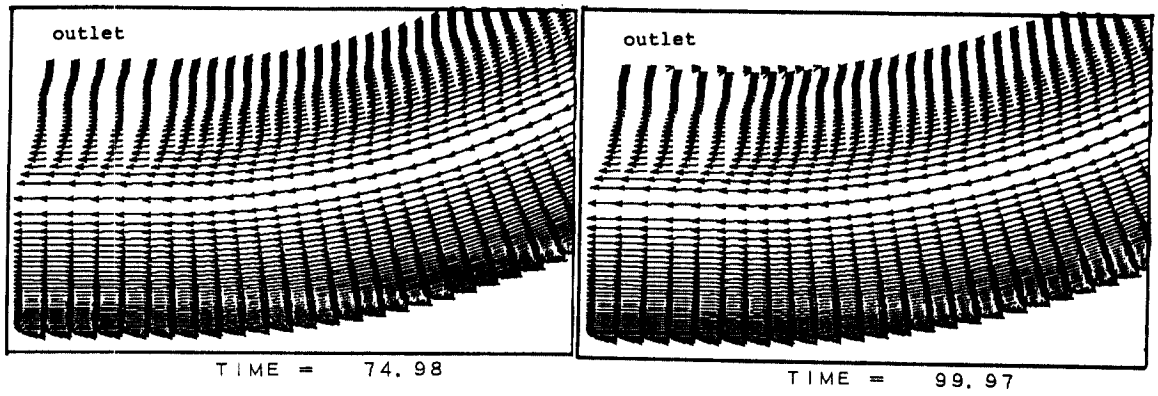

Fig. 18 Time development of velocity distribution near the outlet.

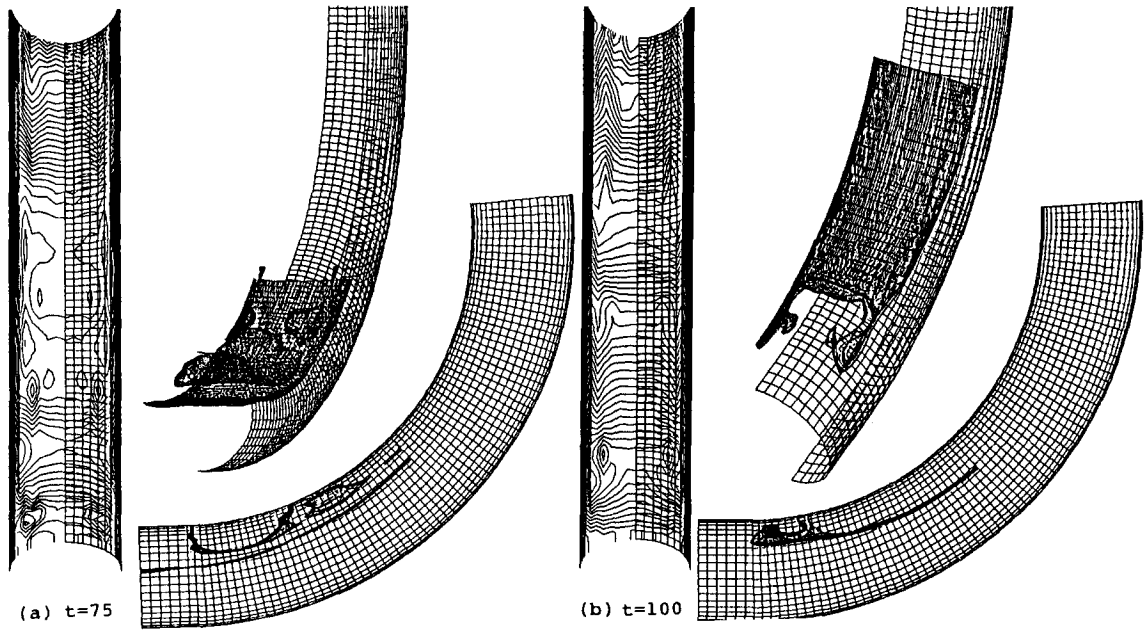

Fig. 19 Pressure contours on the inside wall and equi-pressure surfaces near the outlet

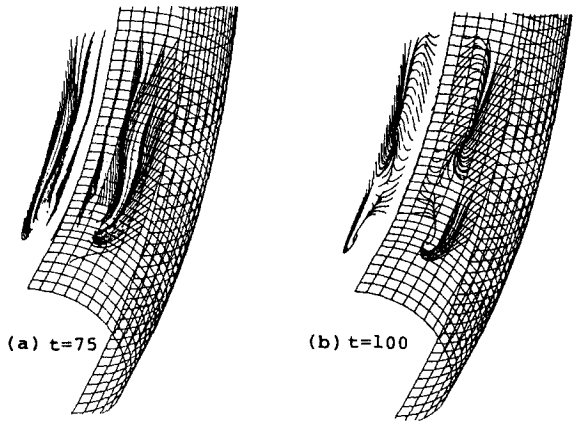

Fig. 20 Computed oil flow pattern

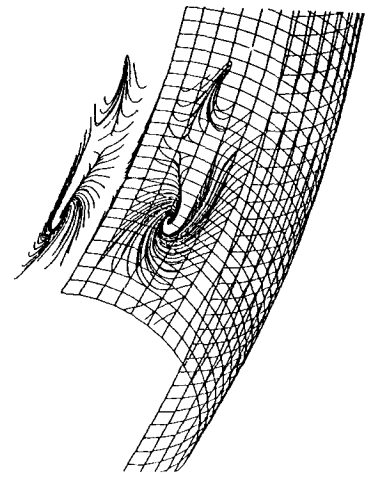

Fig. 22 Computed oil flow pattern.

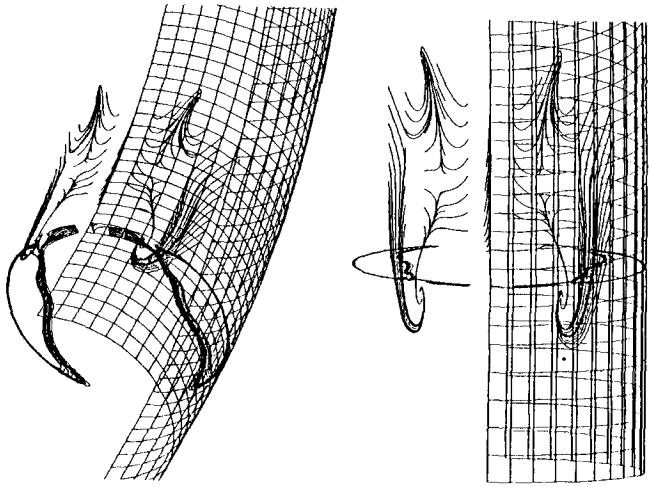

Fig. 21 Computed oil flow pattern and particle paths in a cross-sectional plane.

4. CONCLUSION

In these computations, several different laminar-type solutions have been secured. In low-Dean-number flows, two symmetric recirculating regions appear and such secondary motions induce the separation of cross-sectional flow as the Dean number increases. Moreover, in high-Dean-number flows, the separation of the main flow takes place and the flow field becomes unsteady.

In order to investigate the structure of the secondary flow as well as the main flow, it is highly effective to have comprehesive flow visualization. Without suitable visualization techniques (both hardware and software), we may not be able to understand the physics of these complicated flows.

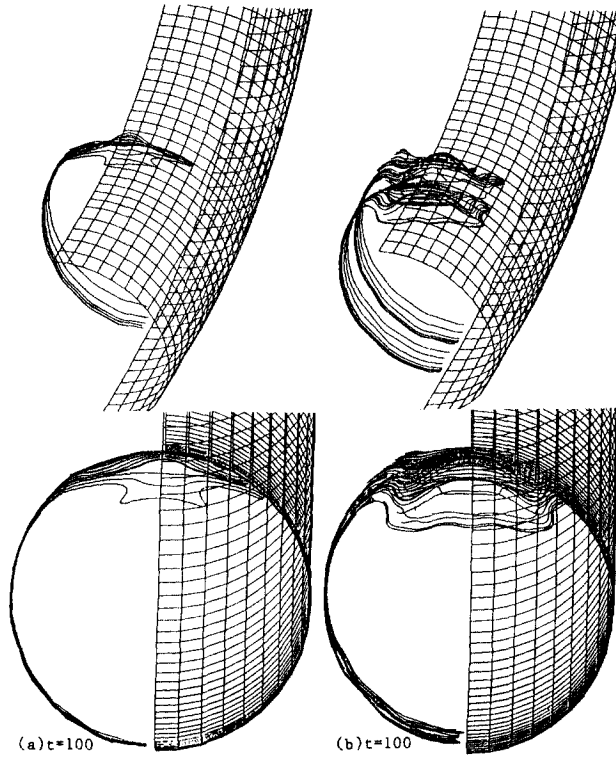

Fig. 23 Vortex lines of an instantaneous vortex structure

REFERENCES

Agrawal, Y., Talbot, L. and Gong, K., 1978, "Laser Anemometer Study of Flow Development in Curved Pipes", Journal of Fluid Mechanics, Vol. 85, pp. 497~518.

Chorin, A.J., 1968, "Numerical Solution of the Navier-Stokes Equation", Mathematical Computation, Vol. 22, pp. 745~765.

Himeno, R., Shirayama, S., Kamo, K. and Kuwahara, K., 1985, "Computational Study of Three-Dimensional Wake Structure", AIAA-8501617.

Humphrey, J.A.C., Iacovides, H. and Launder, B.E., 1985, "Some Numerical Experiments on Developing Laminar Flow in Circular-Sectioned Bends", Journal of Fluid Mechanics, Vol. 154, pp. 357~375.

Kawamura, T. and Kuwahara, K., 1985, "Direct Simulation of a Turbulent Inner Flow by Finite Difference Method", AIAA-85-0376.

Kim, J. and Moin, P., 1986, "The Structure of the Vorticity Field in Turbulent Channel Flow. Part 2. Study of Ensemble-Averaged Fields", Journal of Fluid Mechanics, Vol. 162, pp. 339~363.

Nandakumar, K. and Masliyah, J.H., 1982, "Bifurcation in Steady Laminar Flow Through Curved Tubes", Journal of Fluid Mechanics, Vol. 119, pp. 475~490.

Takami, H. and Kuwahara, K., 1974, "Numerical Study of Three-Dimensional Flow Within a Cubic Cavity", Journal of Physical Society of Japan, Vol. 37, pp. 1695~1705.